INDEPENDENT COMPONENT SEPARATION FROM INCOMPLETE SPHERICAL DATA USING WAVELETS. APPLICATION TO CMB DATA ANALYSIS.

Y. Moudden[1]*, P. Abrial*[1]*, P. Vielva*[3]*, J.-B. Melin*[3]*, J.-L. Starck*[1]*, J.-F. Cardoso*[2]*,*

J. Delabrouille[3] *and M. K. Nguyen*[4]

[1] DAPNIA/SEDI-SAP, CEA/Saclay, F-91191 Gif-sur-Yvette, France, ymoudden@cea.fr
[2] CNRS/ENST, 46 rue Barrault, F-75634 Paris, France, cardoso@tsi.enst.fr
[3] CNRS/PCC, 11 place Marcelin Berthelot, F-75231, Paris, France, delabrouille@cdf.in2p3.fr
[4] CNRS/ENSEA, 6 ave. du Ponceau, F-95014 Cergy-Pontoise, France, nguyen@ensea.fr

ABSTRACT

Spectral matching ICA (SMICA) is a source separation method based on covariance matching in Fourier space that was designed to address in a flexible way some of the general problems raised by Cosmic Microwave Background data analysis. However, a common issue in astronomical data analysis is that the observations are unevenly sampled or incomplete maps with missing patches or intentionally masked parts. In addition, many astrophysical emissions are not well modeled as stationary processes over the sky. These effects impair data processing techniques in the spherical harmonics representation. This paper describes a new wavelet transform for spherical maps and proposes an extension of SMICA in this space-scale representation.

1. INTRODUCTION

In the widely accepted 'Big Bang' model, the Universe started out extremely dense and hot, and then cooled down as it expanded, going through successive phase transitions. Some 370 000 years after the 'Big Bang', when the temperature of the Universe was around 3000 K, a particular transition occurred: as thermal energy was no longer sufficient to keep electrons and positively charged particles apart, these then combined into neutral atoms. Before that, the photons, electrons and light positive nuclei were strongly interacting and the Universe was a highly homogeneous opaque plasma in near thermal equilibrium. Any slight fluctuation in matter density would then also be imprinted in the distribution of photons. After the so-called 'atomic recombination', because photons and atoms interact only very weakly, their fates were no longer so tightly coupled. In fact, the Universe is now transparent and the photons in their majority are and will be moving freely. Since the Universe further expanded, these photons are now in the microwave range but they should still be distributed according to a Black Body emission law, as they were before recombination. They should also still be carrying along information on the density fluctuations in the early Universe from which such large scale structures as galaxies or clusters of galaxies are thought to have evolved *via* gravitational collapse.

The Cosmic Microwave Background (CMB) was first observed in 1965 by Penzias and Wilson confirming a prediction made by Gamow in the late 1940's. But it was not until the early 1990's that evidence for small fluctuations in the CMB sky could finally be found thanks to the observations made by COBE [1]. This was further investigated with higher resolution and sensitivity by a number of experiments among which Archeops [2], and WMAP [3]. Full-sky multi-spectral observations with unprecedented sensitivity and angular resolution are expected from the ESA's PLANCK[1] mission, which is to be launched in 2007.

A major issue in modern cosmology is the measurement of these fluctuations as these are strongly related to the cosmological scenarios describing the properties and evolution of our Universe. In fact, the precise estimation of the statistical properties (spatial power spectrum, Gaussianity) of the CMB field will constrain these models and set tighter bounds on major cosmological parameters describing the matter content and the geometry of our Universe. However, several distinct astrophysical sources emit radiation in the frequency range used for CMB observations [4]. To first order, the total sky emission observed in direction (ϑ, φ) with detector d is a noisy linear mixture of N_c components:

$$x_d(\vartheta,\varphi) = \sum_{j=1}^{N_c} A_{dj} s_j(\vartheta,\varphi) + n_d(\vartheta,\varphi) \qquad (1)$$

where s_j is the emission template for the jth astrophysical process, herein referred to as a *source* or a *component*. The coefficients A_{dj} reflect emission laws while n_d accounts for noise. When observations are obtained from N_d detectors, this equation can be put in vector-matrix form:

$$X(\vartheta,\varphi) = AS(\vartheta,\varphi) + N(\vartheta,\varphi) \qquad (2)$$

where X and N are vectors of length N_d, S is a vector of length N_c, and A is the $N_d \times N_c$ mixing matrix. Hence, estimating the CMB and other component maps from the data

[1] http://astro.estec.esa.nl/Planck

can be seen as a problem of source separation from noisy mixtures that can be approached using blind component separation or independent component analysis (ICA) methods, assuming the astrophysical components originate in independent physical processes.

Blind component separation (and in particular estimation of the mixing matrix) depends very much on the model used for the probability distribution of the sources [5]. In a first set of techniques, source separation is achieved in a noise-less setting, based on the non-Gaussianity of all but possibly one of the components. Methods of this type have been applied to CMB observations in [6, 7]. However, the main component of interest (the CMB itself) is very well described by a Gaussian isotropic stationary model and the observed mixtures suffer from additive gaussian noise, so that better performance can be expected from methods based on Gaussian models.

In a second set of blind techniques, the components are modeled as Gaussian processes, either stationary or non stationary and, in a given representation, separation requires that the sources have diverse, *i.e.* non proportional, variance profiles. The blind separation in a noise free environment, of instantaneous mixtures of non stationary components is examined in [8]. The case of mixed stationary components is studied in [9] : moving to a Fourier representation, it is shown that colored components can be separated based on the diversity of their power spectra. The spectral matching ICA method (SMICA) described in [10, 11], is an extension of this approach to noisy observations.

Although working in the frequency domain does offer several benefits (*e.g.* easy handling of detector dependent point spread functions), the non locality of the spherical harmonics transform will have some undesired effects when dealing with non-stationary components or noise. In fact, in many experiments, only an incomplete sky coverage is available. Either the instrument observes only a fraction of the sky or some regions of the sky must be masked due to localized strong astrophysical sources of contamination: compact radio-sources or galaxies, strong emitting regions in the galactic plane. These effects can be mitigated in a simple manner thanks to the localization properties of wavelets. In fact, building on the above, it is natural to investigate the possible benefits of exploiting both non-stationarity and spectral diversity in a Gaussian model using wavelets. Although blind source separation in the wavelet domain has been previously examined, the setting here is different. We mention, for instance, the separation method in [12] which is based on the non-Gaussianity of the source signals but after a *sparsifying* wavelet transform and the Bayesian approach in [13] which adopts a similar point of view although with a richer source model accounting for correlations in the wavelet representation.

The following section describes a new wavelet transform for data mapped on the sphere. Then, considering the problem of incomplete data as a model case of practical significance, an extension of SMICA for blind source separation in the wavelet representation is discussed in section 3. Numerical experiments are reported in section 4.

2. SPHERICAL WAVELET TRANSFORM

There are clearly many different possible implementations of a wavelet transform on the sphere and their performance depends on the application. We consider here an undecimated isotropic transform. This makes it easy to handle missing patches in observed maps and isotropy is a favorable property when analyzing a statistically isotropic gaussian field such as the CMB, or data sets such as maps of galaxy clusters, which contain only isotropic features [14].

An isotropic transform is obtained using a scaling function $\phi_{l_c}(\vartheta,\varphi)$ with cut-off frequency l_c and azimuthal symmetry, meaning that ϕ_{l_c} does not depend on the azimuth φ. Hence its spherical harmonic coefficients $\widetilde{\phi}_{l_c}(l,m)$ vanish when $m \neq 0$ so that :

$$\phi_{l_c}(\vartheta,\varphi) = \phi_{l_c}(\vartheta) = \sum_{l=0}^{l=l_c} \widetilde{\phi}_{l_c}(l,0) Y_{l0}(\vartheta,\varphi) \tag{3}$$

Then, convolving a map $s_0(\vartheta,\varphi)$ with ϕ_{l_c} is greatly simplified and the spherical harmonic coefficients of the resulting map s_1 are readily given by

$$\widetilde{s}_1(l,m) = \sqrt{\frac{2l+1}{4\pi}} \widetilde{\phi}_{l_c}(l,0) \widetilde{s}_0(l,m) \tag{4}$$

and this is taken advantage of in the present implementation. The spherical harmonic coefficients of the scaling function we retained here ϕ_{l_c} follow a cubic B-spline profile:

$$\widetilde{\phi}_{l_c}(l,0) = \frac{2}{3} B_3(\frac{2l}{l_c}) \tag{5}$$

$$\tag{6}$$

where B_3 is defined for $x \in [-2,2]$ by

$$\begin{aligned} B_3(x) = & \frac{1}{12}(\mid x-2 \mid^3 - 4 \mid x-1 \mid^3 + 6 \mid x \mid^3 \\ & - 4 \mid x+1 \mid^3 + \mid x+2 \mid^3) \end{aligned} \tag{7}$$

and null elsewhere.

Assuming, for ease of presentation, that s_0 is actually related to an unknown map s_{-1} by

$$s_0 = s_{-1} * \phi_{l_c} \tag{8}$$

where $*$ stands for convolution, a sequence of recursively smoother approximations to s_0 on a dyadic resolution scale can be obtained as follows

$$\begin{aligned} s_1 &= s_{-1} * \phi_{2^{-1} l_c} = s_0 * h_{l_c} \\ s_2 &= s_{-1} * \phi_{2^{-2} l_c} = s_1 * h_{2^{-1} l_c} \\ &\dots \\ s_j &= s_{-1} * \phi_{2^{-j} l_c} = s_{j-1} * h_{2^{-j+1} l_c} \end{aligned} \tag{9}$$

where $\phi_{2^{-j} l_c}$ is a rescaled version of ϕ_{l_c} and the $h_{2^{-j} l_c}$ are low pass filters defined by :

$$h_{2^{-j} l_c} = \begin{cases} \frac{\phi_{2^{-j-1} l_c}}{\phi_{2^{-j} l_c}} & \text{if } l < \frac{l_c}{2^{j+1}} \\ 0 & \text{otherwise} \end{cases} \tag{10}$$

The cut-off frequency is reduced by a factor of 2 at each step so that in applications where this is useful such as compression, the number of samples could be reduced by the same factor. Here however, no downsampling is performed and the maps have the same number of pixels on each scale. Hence the orthogonality constraint is clearly relaxed, so there is some freedom in the choice of the wavelet function ψ_{l_c} to be used with the scaling function ϕ_{l_c}. Taking the difference between two consecutive smooth approximations is a simple possibility which results in the following construction of the wavelet function

$$\psi_{2^{-j}l_c} = \phi_{2^{-j+1}l_c} - \phi_{2^{-j}l_c} \tag{11}$$

and, defining $g_{2^{-j}l_c} = 1 - h_{2^{-j}l_c}$, the detail maps or wavelet coefficients at scale j are given by :

$$\begin{aligned} s_j^w &= s_{j-1} - s_j = \psi_{2^{-j}l_c} s_{-1} \\ &= s_{j-1} * g_{2^{-j+1}l_c} \end{aligned} \tag{12}$$

This particular decomposition is readily inverted by

$$s_0(\vartheta,\varphi) = s_J(\vartheta,\varphi) + \sum_{j=1}^{J} s_j^w(\vartheta,\varphi) \tag{13}$$

which is a simple addition of the smooth array with the detail maps.

3. SMICA IN WAVELET SPACE

Spectral matching ICA is a blind source separation technique which, unlike most standard ICA methods, is able to recover Gaussian sources from noisy observations. It operates in the spectral domain and is based on *spectral diversity*: it is able to separate sources provided they have different power spectra. A detailed derivation can be found in [11]. We focus here on extending SMICA to the wavelet domain using the transform described above. We refer to this extension as wSMICA.

Consider the linear mixture model (2): applying the above wavelet transform on both sides does not affect the mixing matrix A. Then, assuming independent source and noise processes, the covariance matrix of the observations at scale j , is structured as

$$R_{\mathbf{W},X}(j) = A R_{\mathbf{W},S}(j) A^\dagger + R_{\mathbf{W},N}(j) \tag{14}$$

where $R_{\mathbf{W},S}(i)$ and $R_{\mathbf{W},N}(i)$ are the diagonal spectral covariance matrices in the wavelet representation of S and N respectively. Provided estimates $\widehat{R}_{\mathbf{W},X}(j)$ of $R_{\mathbf{W},X}(j)$ can be obtained from the data, our wavelet-based version of SMICA consists in minimizing the wSMICA criterion:

$$\Phi(\theta) = \sum_{j=1}^{J+1} \alpha_j \mathcal{D}\left(\widehat{R}_{\mathbf{W},X}(j),\, A R_{\mathbf{W},S}(j) A^\dagger + R_{\mathbf{W},N}(j)\right) \tag{15}$$

for some sensible choice of the weights α_i and of the matrix mismatch measure $\mathcal{D}$, with respect to the full set of parameters $\theta = (A, R_{\mathbf{W},S}(j), R_{\mathbf{W},N}(j))$ or a subset thereof. As discussed in [11], a good choice for $\mathcal{D}$ is

$$\mathcal{D}_{KL}(R_1, R_2) = \frac{1}{2}\Big(\mathrm{tr}(R_1 R_2^{-1}) - \log\det(R_1 R_2^{-1}) - m\Big) \tag{16}$$

which is the Kullback-Leibler divergence between two m-variate zero-mean Gaussian distributions with covariance matrices R_1 and R_2. With this mismatch measure, the SMICA is shown to be related to the likelihood of the data in a Gaussian model so that we can resort to the EM algorithm to minimize (15). Actually, starting with the EM algorithm and finishing with a few BFGS steps was found to be a much faster strategy [11].

In dealing with non stationary data or, as a special case, with gapped data, an attractive feature of wavelet filters over the spherical harmonic transform is that they are well localized in the initial representation. Provided the wavelet filter response on scale j is short enough compared to data size and gap widths, most of the samples in the filtered signal will then be unaffected by the presence of gaps. Hence using exclusively these samples yields an estimated covariance matrice $\widehat{R}_{\mathbf{W},X}(j)$ which is not biased by the missing data, although at the cost of a slight increase of variance due to discarding some data samples. Writing the wavelet decomposition on J scales of X as

$$X(\vartheta,\varphi) = X_J(\vartheta,\varphi) + \sum_{j=1}^{J} X_j^w(\vartheta,\varphi) \tag{17}$$

and denoting l_j the size of the set $\mathcal{M}_j$ of wavelet samples unaffected by the gaps at scale j, the wavelet covariances are simply estimated using

$$\begin{aligned} \widehat{R}_{\mathbf{W},X}(1 \le j \le J) &= \frac{1}{l_j} \sum_{t\in\mathcal{M}_j} X_j^w(\vartheta_t,\varphi_t) X_j^w(\vartheta_t,\varphi_t)^\dagger \\ \widehat{R}_{\mathbf{W},X}(J+1) &= \frac{1}{l_{J+1}} \sum_{t\in\mathcal{M}_{J+1}} X_{J+1}(\vartheta_t,\varphi_t) X_{J+1}(\vartheta_t,\varphi_t)^\dagger \end{aligned} \tag{18}$$

The weights in the spectral mismatch (15) should be chosen to reflect the variability of the estimate of the corresponding covariance matrix. Since wSMICA uses wavelet filters with only limited overlap, in the case of complete data maps, we follow the derivation in [11] and take α_j to be proportional to the number of spherical harmonic modes in the spectral domain covered at scale j. In the case of data with gaps, we must further take into account that only a fraction β_i of the wavelet coefficients are unaffected so that the α_j should be modified in the same ratio.

When running wSMICA, power densities in each scale are obtained for the sources and detector noise along with the estimated mixing matrix. These are used in reconstructing the source maps *via* Wiener filtering in each scale: a coefficient

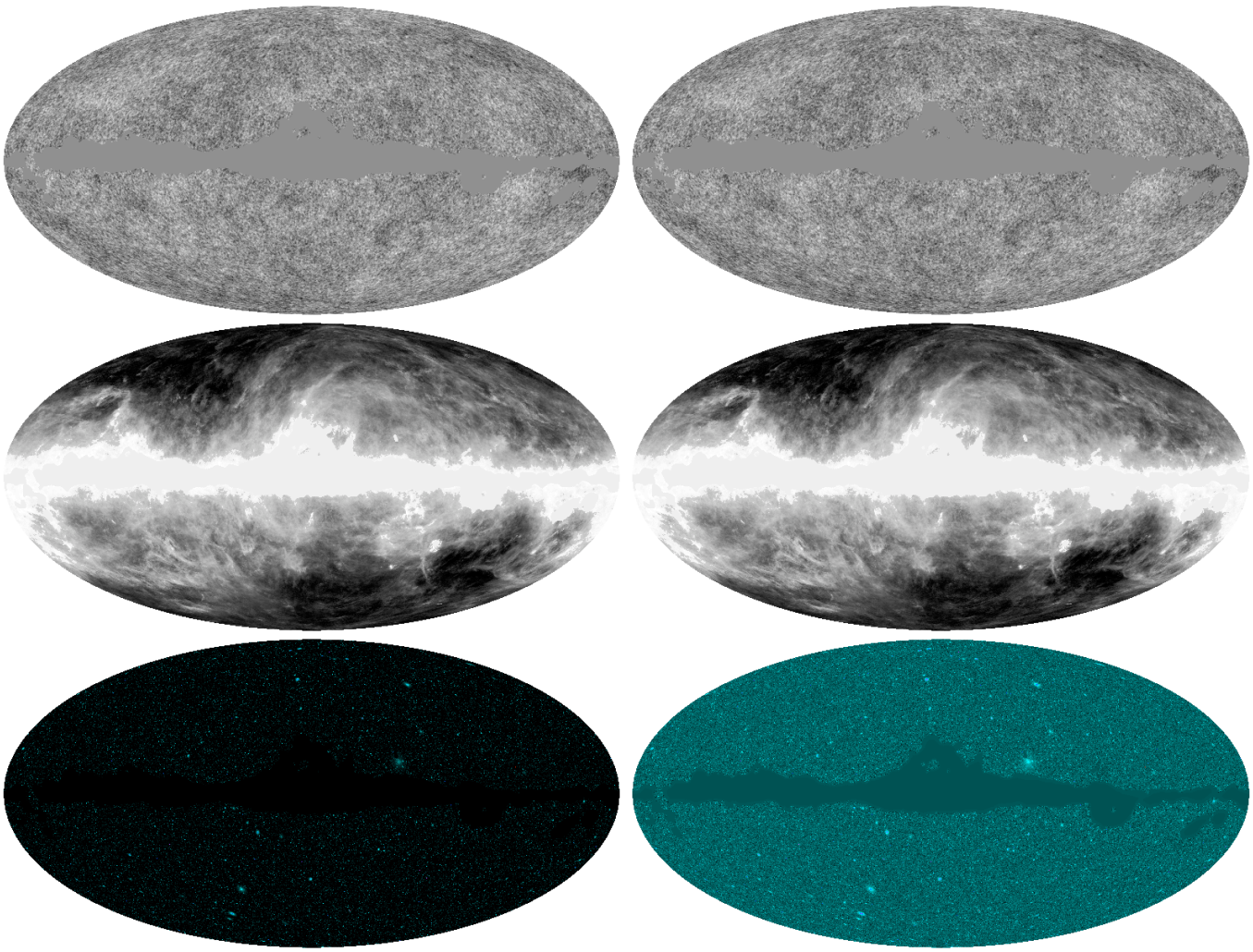

Fig. 1. The maps on the left are the templates for CMB, galactic dust and SZ used in the experiment described in section 4. The maps on the right were estimated using wSMICA and scalewise Wiener filtering. (The different maps are drawn here in different color scales in order to enhance structures and ease visual comparisons).

$X_j^w(\vartheta,\varphi)$ is used to reconstruct the maps according to

$$\widehat{S}_j^w(\vartheta,\varphi) = \big(\widehat{A}^\dagger \widehat{R}_{\mathbf{W},N}(j)^{-1}\widehat{A} + \widehat{R}_{\mathbf{W},S}(j)^{-1}\big)^{-1} \times \widehat{A}^\dagger \widehat{R}_{\mathbf{W},N}(j)^{-1} X_j^w(\vartheta,\varphi) \quad (19)$$

In the limiting case where noise is small compared to signal components, this filter reduces to

$$\widehat{S}_j^w(\vartheta,\varphi) = (\widehat{A}^\dagger \widehat{R}_{\mathbf{W},N}(j)^{-1}\widehat{A})^{-1}\widehat{A}^\dagger \widehat{R}_{\mathbf{W},N}(j)^{-1} X_j^w(\vartheta,\varphi) \quad (20)$$

Clearly, the above Wiener filter is optimal only in front of stationary Gaussian processes. For non Gaussian maps, such as given by the Sunyaev Zel'dovich effect (defined in the next section), better reconstruction can be expected from non linear methods.

4. NUMERICAL EXPERIMENTS

The application of wSMICA to synthetic mixtures of CMB, galactic dust and Sunyaev Zel'dovich (SZ) maps is considered here. Dust emission is the greybody emission of small dust particles in our own galaxy. The intensity of this emission is strongly concentrated towards the galactic plane, although cirrus clouds at high galactic latitudes are present as well [15]. The SZ effect is a small distortion of the CMB blackbody emission that can be modeled, to first order, as a small additive emission, negative at frequencies below 217 GHz, and positive at frequencies above [16].

The component maps used, shown on figure 1, were obtained as described in [11]. The problem of instrumental point spread functions is not adressed here, and all maps are assumed to have the same resolution. The high level foreground emissions from the galactic plane region were discarded using the $Kp2$ mask from the WMAP team website[2]. These three *incomplete* maps were mixed using the matrix in table 1 to simulate observations in the six channels of the Planck high frequency instrument (HFI).

CMB	DUST	SZ	channel
1.0	1.0	-1.51	100 GHz
1.0	2.20	-1.05	143 GHz
1.0	7.16	0.0	217 GHz
1.0	56.96	2.22	353 GHz
1.0	1.1×10^3	5.56	545 GHz
1.0	1.47×10^5	11.03	857 GHz

Table 1. Entries of A, the mixing matrix used in our simulations.

Gaussian *instrumental* noise was added in each channel according to model (2). The relative noise standard deviations between channels were set according to the nominal values of the Planck HFI given in table 2 and we experimented with five *global* noise levels at -6, -3, 0, $+3$ and $+6$ dB from nominal values.

[2] *http://lambda.gsfc.nasa.gov/product/map/intensity_mask.cfm*

100 GHz	143 GHz	217 GHz	channel
2.65×10^{-6}	2.33×10^{-6}	3.44×10^{-6}	noise std
353 GHz	545 GHz	857 GHz	channel
1.05×10^{-5}	1.07×10^{-4}	4.84×10^{-3}	noise std

Table 2. Nominal noise standard deviations in the six channels of the Planck HFI.

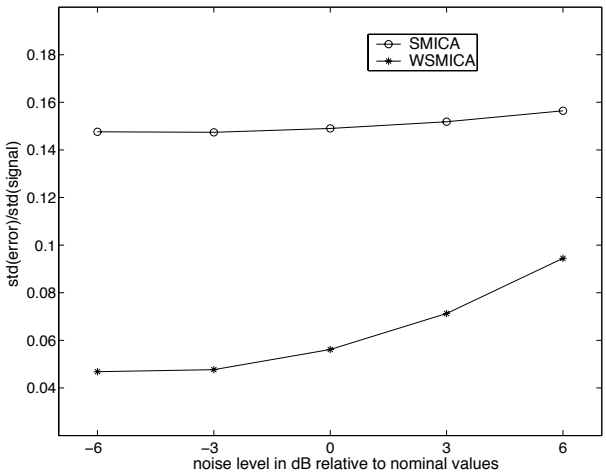

Fig. 2. Relative reconstruction error defined by (21) of the CMB component map using SMICA and wSMICA as a function of the instrumental noise level.

The synthetic observations were decomposed into six scales using our wavelet transform on the sphere and wSMICA was used to obtain estimates of the initial source templates. For the sake of comparison, a separation with SMICA was also performed based on Fourier statistics computed in the same six dyadic bands imposed by our choice of wavelet transform.

The resulting component maps estimated using wSMICA, for nominal noise levels, are shown on figure 1 where the quality of reconstruction can be visually assessed by comparison to the initial components. Figure 2 gives more quantitative results in the particular case of CMB, comparing the performance of SMICA and wSMICA in terms of reconstruction error MQE which we defined by

$$MQE = \frac{\mathbf{std}(CMB(\vartheta,\varphi) - \alpha \times \widehat{CMB}(\vartheta,\varphi))}{\mathbf{std}(CMB(\vartheta,\varphi))} \quad (21)$$

where $\mathbf{std}$ stands for empirical standard deviation (obviously computed outside the masked regions), and α is a linear regression coefficient estimated in the least squares sense. These results clearly show that using wavelet-based covariance ma-

trices provides a simple and efficient way to cancel the bad impact that gaps actually have on the performance of estimation using Fourier based statistics. Another way in which the effect of the gap on the performance of SMICA could probably be reduced, is by applying a proper apodizing window on the data prior to estimating the spectral covariance, which is standard practice in harmonic analysis. With the mask used, building such a window is not straightforward so that, in the present experiments, SMICA was applied without correction for the gaps. The results given on figure 2 should be interpreted knowingly.

It may be argued that the proposed wavelet based approach, as implemented with wavelet transform described in section 2, offers little flexibility in the spectral bands available for wSMICA while the Fourier approach gives complete flexibility in this respect. But actually it is possible to use other transforms on the sphere (e.g. wavelet packet transform, *continuous* wavelet transform) or in fact any set of linear filters preferably well localized both on the sphere and in the spherical harmonics domain. This way gaps are well dealt with and spectral information is preserved to achieve the source separation objective.

5. CONCLUSION

This paper has presented a new wavelet transform for data mapped to the sphere. This transform was used to extend the Spectral Matching ICA method to the wavelet domain, motivated by the need to deal with non stationary components. Maps with missing patches are a particular example of practical significance. Our numerical experiments, based on realistic simulations of the astrophysical data expected from the Planck mission, clearly show the benefits of correctly processing existing gaps in the data which is not a real surprise. We showed that, moving to the wavelet domain, it is possible to easily cope with gaps of any shape in a very simple manner, while still retaining spectral information for component separation. Clearly, other possible types of non-stationarities in the collected data such as spatially varying noise or component variance, etc. could be dealt with very simply in a similar fashion using our wavelet extension of SMICA.

Acknowledgements - We are thankful to the Healpix team for allowing us to use their software package[3].

6. REFERENCES

[1] G. F. Smoot et al., "Structure in the COBE differential microwave radiometer first-year maps", *Astrophysical Journal Letters*, vol. 396, pp L1-L5, 1992.

[2] A. Benoit et al., "Archeops: a high resolution, large sky coverage balloon experiment for mapping cosmic microwave background anisotropie", *Astroparticle Physics*, vol. 17, no 2, pp 101-124, 2002.

[3] C. L. Bennett et al., "First year Wilkinson microwave anisotropy probe (Wmap) observations: preliminary maps and basic results", *Astrophysical Journal Supplement*, vol. 148, pp 1-27, 2003.

[4] F. Bouchet and R. Gispert, "Foregrounds and CMB experiments: Semi-analytical estimates of contamination", *New Astronomy*, vol. 4, pp 443-479, 1999.

[5] J.-F. Cardoso, "The three easy routes to independent component analysis; contrasts and geometry", *Proc. ICA2001 Workshop*, San Diego, 2001.

[6] C. Baccigalupi, L. Bedini et al., "Neural networks and separation of cosmic microwave background and astrophysical signals in sky maps", *Mon. Not. R. Astron. Soc.*, vol. 318, no 3, pp 769-780, 2000.

[7] D. Maino, A. Farusi et al., "All-sky astrophysical component separation with Fast Independent Component Analysis (FASTICA)", *Mon. Not. R. Astron. Soc.*, vol. 334, no 1, pp 53-68, 2002.

[8] D.-T. Pham and J.-F. Cardoso, "Blind separation of instantaneous mixtures of non stationary sources", *IEEE Tr. Sig. Proc.*, vol. 49, no. 9, pp 1837-1848, 2001.

[9] D. T. Pham, "Blind Separation of Instantaneous Mixture of Sources via the Gaussian Mutual Information Criterion", *Signal Processing*, vol. 81, pp 855-870.

[10] J.-F. Cardoso, H. Snoussi et al., "Blind separation of noisy Gaussian stationary sources. Application to cosmic microwave background imaging", *Proc. EUSIPCO2002*, pp 561-564, Toulouse (France), 2002.

[11] J. Delabrouille, J.-F. Cardoso and G. Patanchon, "Multidetector multi-component spectral matching and application for CMB data analysis", *Mon. Not. R. Astron. Soc.*, vol. 346, no 4, pp 1089-1102, 2003.

[12] M. Zibulevsky and B. Pearlmutter, "Blind source separation by sparse decomposition in a signal dictionary", *Neural Computations*, vol. 13, no 4, pp 863-882, 2001.

[13] M. Ichir and A. Mohammad-Djafari, "Wavelet Domain Blind Image Separation", *Proc. of SPIE, Mathematical Modeling, Wavelets X*, San Diego, 2003.

[14] J.-L. Starck, F. Murtagh and A. Bijaoui, *Image and Data Analysis : The multiscale approach*, Cambridge University Press, 1998.

[15] D., J. Schlegel, D. P. Finkbeiner and M. Davis, "Maps of Dust Infrared Emission for Use in Estimation of Reddening and Cosmic Microwave Background Radiation Foreground", *Astrophysical Jouranl*, vol. 500, pp 525, 1998.

[16] M. Birkinshaw, "The Sunyaev-Zel'dovich effect", *Physics Reports*, no 310, pp 97-195, 1999.

[3] *http://www.eso.org/kgorski/healpix/*